

# ACCURACY AND RADIOMETRIC STUDY ON VERY HIGH RESOLUTION DIGITAL CAMERA IMAGES

R. Passini\*, K. Jacobsen\*\*

\*BAE SYSTEMS GP&S  
124 Gaither Dr., Suite 100, Mount Laurel, NJ 08054, USA  
Ricardo.Passini@baesystems.com

\*\*Institute of Photogrammetry and Geoinformation  
Leibniz University Hannover  
jacobsen@ipi.uni-hannover.de

**KEY WORDS:** digital camera, block adjustment, self calibration, accuracy; resolution

## ABSTRACT:

A test area close to Philadelphia, USA, has been flown with an UltraCamX from the extreme low flying elevation of 310m above ground. This leads to images with 22mm ground sampling distance (GSD). The required end lap of 60% corresponds just to 84m. The imaging sequence of the UltraCamX with 1.6sec enables with the minimal flying speed of 220km/hour only a base of 98m, by this reason each flight line was flown twice in the same direction at 20 % end lap. In this way combining the 2 flights per strip a 60% end lap was achieved. The area is covered also at 60% lateral overlap. 44 targeted ground control points with a standard deviation of the coordinate components of 1.5cm and better are available in the 210 used images.

An automatic aerial triangulation with LPS has been made. Detailed analysis with the Hannover program for bundle block adjustment BLUH showed systematic image errors requiring an improvement of the UltraCam-specific additional parameters. Finally by bundle adjustment with self calibration a standard deviation of the horizontal check point coordinates of approximately 14mm corresponding to 0.6 GSD and in Z up to 26mm corresponding to 1.2 GSD has been reached for the check points measured in the average in 6 images. This extreme accuracy is limited by the identification and the accuracy of the ground control and check points.

The TDI was able to compensate the very fast forward motion; no obvious reduced image quality in flight direction could be seen. Radiometric image quality for these high resolution images were also conducted by assessing the image quality in terms of edge analysis. This allows the determination of the effective resolution for the panchromatic and the pan-sharpened images.

## 1. INTRODUCTION

In several countries digital aerial cameras have replaced analogue photogrammetric cameras. With large size digital frame cameras new imaging possibilities exist. The electronic forward motion compensation (FMC) by transfer delay integration (TDI) is faster as the manual FMC, allowing extreme flight conditions of just 310m above ground. Of course the radiometric and geometric image quality has to be checked for such an extreme situation where the aircraft is operated in a very turbulent atmosphere. So not only a loss of resolution may be caused by not totally perfect TDI-movement, which varies stronger for such a large scale, also a lateral image movement caused by roll may be available.

elevation during imaging was in the range of 24°. Panchromatic and pan-sharpened RGB-images are available.

## 2. USED TEST DATA

Organized by BAE SYSTEMS, Mt Laurel, NJ, USA, a photo flight with Microsoft Vexcel Imaging UltraCamX over the test field Franklin Mills has been made. 44 control points with a standard deviation of the coordinate components not exceeding 1.5cm are available. Based on the repeated flight with projection centers shifted half a base length, the block has approximately 60% end and 60% side lap (fig. 1). With a flying height above ground of 310m the minimal imaging rate of 1.6 sec corresponds to a minimal base of 98m at the lowest flight speed of 220 km/h, exceeding the base for 60% endlap of 83m and requiring the repeated flight over the same strip. The sun

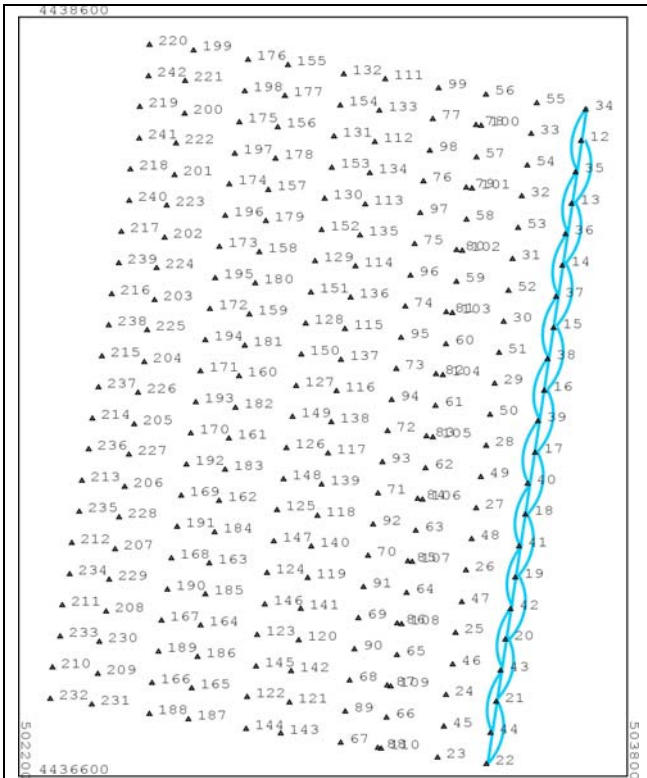


Fig. 1: block configuration based on repeated flight, shifted half a base length as shown on right hand side

### 3. RADIOMETRIC QUALITY

The effective resolution has been checked by edge analysis (see also Passini, Jacobsen 2008). With similar sun elevation the flight in 2007 over the Franklin Mills test field with 37mm GSD showed for the UltraCamX in the center of panchromatic images a factor for the effective pixel size of 1.03, that means nearly no loss of image quality of the effective against the nominal GSD. In the image corners pan-sharpened images showed a factor for the effective pixel size of 1.23 – this corresponds to the information about the resolution available in the calibration certificate. Pan-sharpened images showed with a factor of 1.23 an overall loss of image quality over the whole area.



Fig. 2: pick up in pan-sharpened image with 2.2cm GSD



Fig. 3: light pole and power line with 2.2cm GSD



Fig. 4: manhole with 2.2cm GSD

The images of the high resolution flight have been improved by edge enhancement – in most cases this will be done for digital images. The edge enhancement influences the edge analysis, leading to a smaller factor for the effective pixel size.



Fig. 5: traffic separator

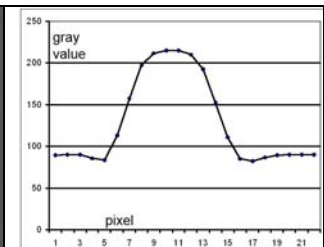


Fig. 6: gray value cross-section through traffic separator

The effect of the edge enhancement can be seen in figure 5 at the dark area surrounding the bright parts and in the cross-section, shown in figure 6. The typical effect of the edge enhancement is the reduction of the grey values in front of the raise to the brighter parts. The typical effect of edge enhancement with darker lines beside brighter parts can also be seen at the pick up in figure 2.

Under the condition of the edge enhancement the factor for the effective pixel size for the panchromatic image in the average is 1.12 without significant change to the image corners and without dependency upon the orientation of the edge. That means an effect of the image movement cannot be seen; on the other hand the resolution is in general reduced a little, which may also be caused by turbulent atmosphere. The factor of 1.12 means, the effective GSD is 22mm x 1.12 = 24.6mm. The pan-

sharpened images show in the average a factor for the effective pixel size of 1.14, not being significantly larger as for the panchromatic image. This was different for the flight in 2007, where the pan-sharpened images showed a factor of 1.23. Only the red channel of the pan-sharpened image shows in the corner a factor of 1.22, for blue and green this could not be seen. By theory for the longer wavelength of the red color such an effect can be explained. Of course the factor for the effective pixel also depends upon the used diaphragm that means it can be different for different flights

#### 4. GEOMETRIC QUALITY

An automatic aero triangulation with LPS has been made. In the average 303 tie points per image or between 122 and 466 points per image have been determined. The image points are nearly equally distributed (fig. 7); the variation in the distribution is caused by the overlap of neighbored images.

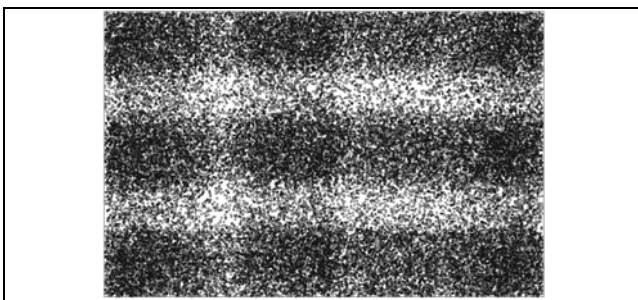


Fig. 7: distribution of points in the images – overlay of all 63623 image points

Nevertheless caused by changing object contrast the number of images per object point is varying in the block (fig. 8). In the centre left, upper left and on right hand side there are areas with just few tie points, but this is not causing problems for the block geometry.

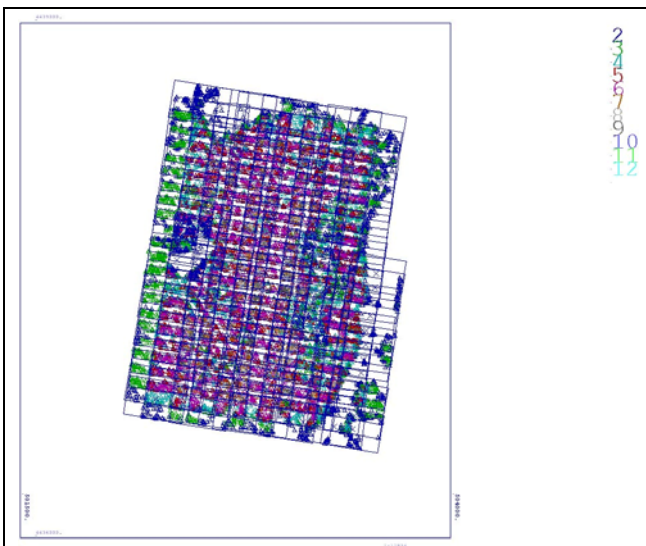


Fig. 8: block configuration with all used images, object points colored by number of images/point – color coding see upper right

For the analysis of the image geometry block adjustments without additional information as projection centers determined by GPS or attitude information have been made. On the reached accuracy level the direct sensor orientation was not precise

enough for supporting the block adjustment. The image geometry can be analyzed by means of the residuals. The residuals (remaining discrepancies at the image coordinates) can be overlaid corresponding to the image coordinates. If all more than 63000 residuals are overlaid and averaged in small image sub-areas, they are indicating systematic image errors – the discrepancy of the real image geometry against the mathematical model of perspective geometry. The independent computed vectors are strongly correlated with neighbored vectors, confirming existing systematic image errors (fig. 9).

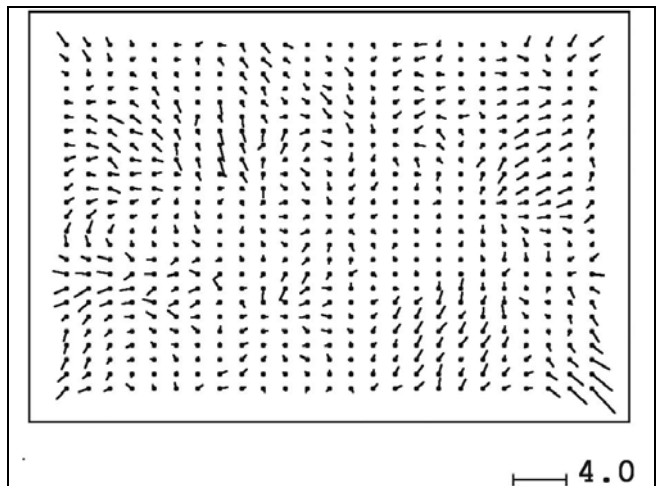


Fig. 9: overlaid and averaged image coordinate residuals of block adjustment without self calibration,  $RMS_x=0.89\mu m$ ,  $RMS_y=1.42\mu m$

The overlaid and averaged image coordinate residuals of a block adjustment without self calibration, shown in figure 9, are indicating systematic image errors, which can be determined by block adjustment with self calibration by additional parameters. The analysis has been done with the Hannover program system for bundle block adjustment BLUH. In BLUH a set of additional parameters dominated by physical justification is used (Jacobsen 2007). For standard photos a set of 12 additional parameters is satisfying. The special geometry of the UltraCam, based on a combination of 9 CCD-matrixes from 4 sub-cameras, can be respected with 32 UltraCam-specific additional parameters. With the parameters 42 up to 73 shifts in x and y, scale changes and perspective deformation of the 8 CCD-arrays in relation to the centre part can be determined – these parameters have been refined against the former set used for example in Passini, Jacobsen 2008. In general the introduced additional parameters are checked for their justification and not justified additional parameters are not used for the final adjustment. So even if the 32 UltraCam-specific and the 12 basic parameters are introduced, the final block adjustment will not be made with 44 additional parameters – in most cases of this data set approximately 34 additional parameters have been used if 44 parameters have been chosen.

The overlaid and averaged image coordinate residuals are nearly independent upon the number of used control points, by this reason they are only shown for the block adjustment with 21 control points. A bundle block adjustment with the standard 12 additional parameters of program system BLUH could not eliminate the systematic errors shown by the overlaid and averaged image coordinate residuals (fig. 11), also with the basic 12 additional parameters plus the UltraCam-specific parameters the systematic image errors could not be removed totally (fig. 12).

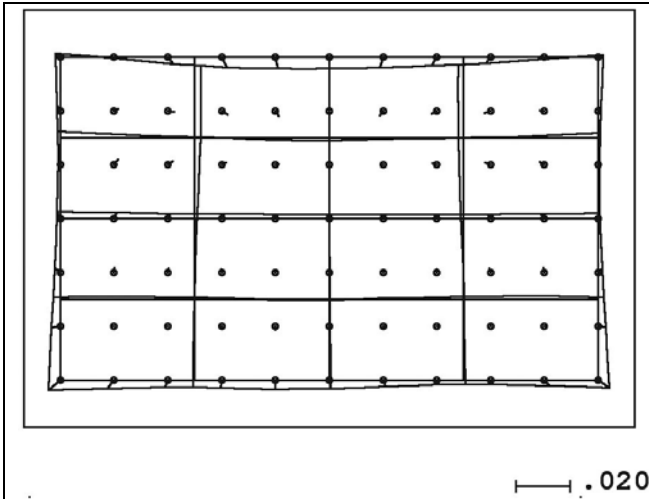


Fig. 10: systematic image errors of adjustment with basic set of additional parameters 1-12

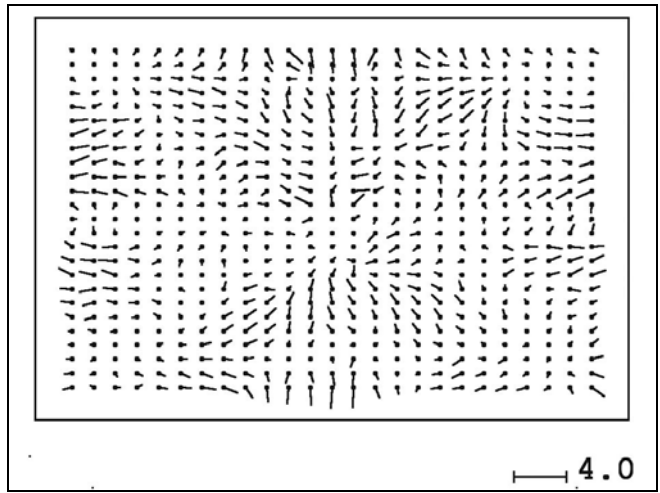


Fig. 13: overlaid and averaged image coordinate residuals of block adjustment with additional parameters 1-12 + 42-73,  $RMS_x=0.84\mu m$ ,  $RMS_y=1.25\mu m$

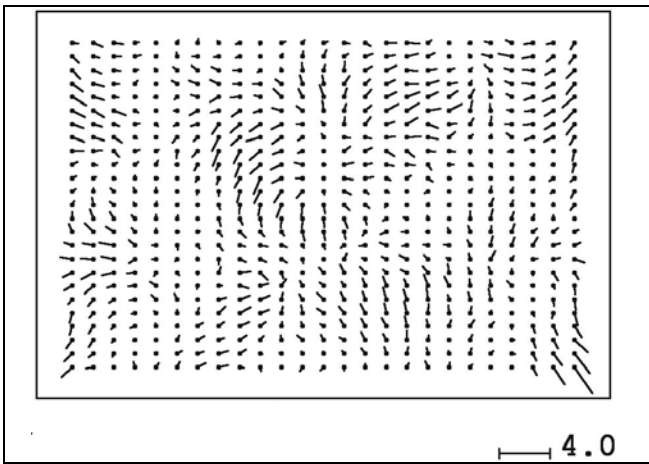


Fig. 11: overlaid and averaged image coordinate residuals of block adjustment with additional parameters 1-12,  $RMS_x=0.84\mu m$ ,  $RMS_y=1.25\mu m$

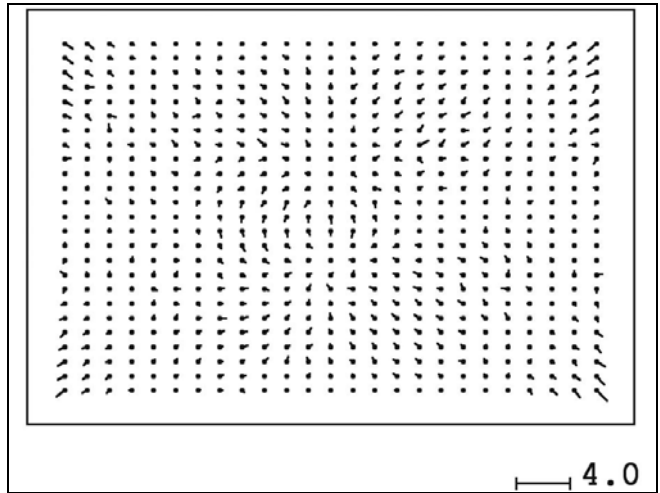


Fig. 14: overlaid and averaged image coordinate residuals of block adjustment with additional parameters 1-12 + 3 iterations with iteratively improved image coordinates

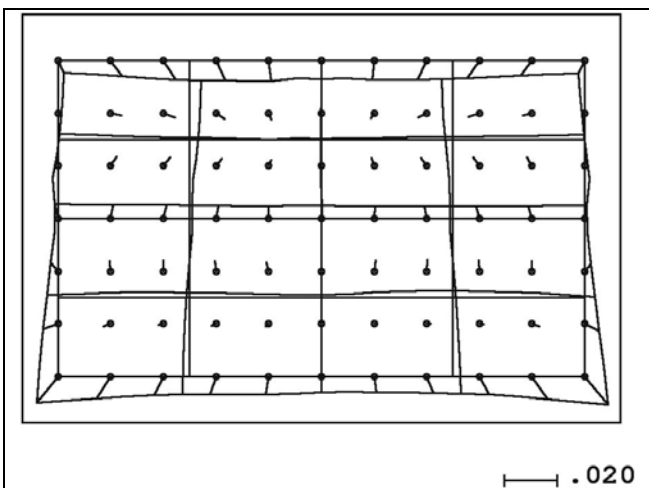


Fig. 12: systematic image errors of adjustment with additional parameters 1-12 + UltraCam-specific parameters 42-73

Only with an iterative improvement of the image coordinates by the overlaid and averaged image coordinate residuals the remaining systematic errors could be minimized (fig. 14). This iterative improvement reduced the  $\sigma_0$  to  $1.16\mu m$ , but it did not improve the discrepancies at the control and check points only in the case of 8 control points, for a higher number of control points it did not improve the results.

8 control points are not a satisfying number of control points for a block adjustment not supported by direct sensor orientation (see also table 1). Especially at the sensitive height component this can be seen. With an additional control point in the block center (fig. 16) the block adjustment was satisfying. Especially for the vertical component the self calibration with additional parameters is absolutely required, while the UltraCam-specific parameters and the iterative adjustment with improving the systematic image errors by the overlaid and averaged residuals have reduced the  $\sigma_0$ , but not significantly the discrepancies at the independent check points. Of course this may be caused by the limited accuracy of the control and check points which are specified as better than 1.5cm – the root mean square discrepancies at the check points are in this range.



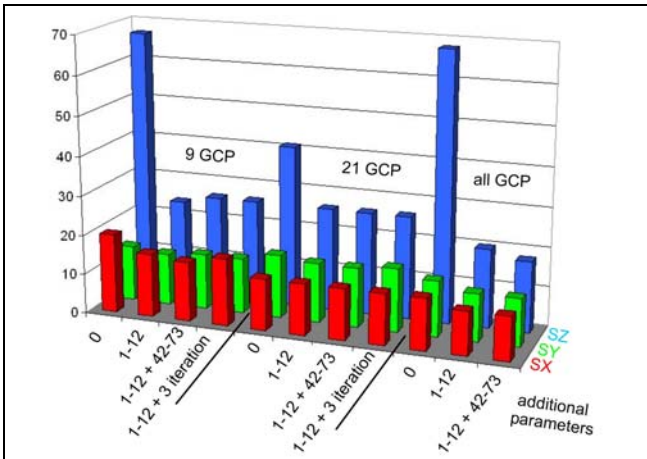


Fig. 15: graphical presentation of RMS discrepancies at independent check points – in case of all GCP: RMS at control points

|                                   |      | RMSX | RMSY | RMSZ | Sigma0 |
|-----------------------------------|------|------|------|------|--------|
| 8 GCP<br>no AP                    | GCPs | 14   | 11   | 71   | 1.57μm |
|                                   | CP   | 23   | 15   | 375  |        |
| 8 GCP<br>AP 1-12                  | GCPs | 5    | 8    | 13   | 1.44μm |
|                                   | CP   | 18   | 14   | 39   |        |
| 8 GCP<br>AP 1-12 +<br>42-73       | GCPs | 4    | 8    | 13   | 1.25μm |
|                                   | CP   | 17   | 13   | 38   |        |
| 8 GCP<br>AP 1-12+<br>3 iteration  | GCPs | 4    | 9    | 12   | 1.19μm |
|                                   | CP   | 18   | 14   | 27   |        |
| 9 GCP<br>no AP                    | GCPs | 9    | 10   | 60   | 1.60μm |
|                                   | CP   | 20   | 14   | 67   |        |
| 9 GCP<br>AP 1-12                  | GCPs | 5    | 9    | 11   | 1.45μm |
|                                   | CP   | 16   | 13   | 24   |        |
| 9 GCP<br>AP 1-12 +<br>42-73       | GCPs | 5    | 8    | 11   | 1.26μm |
|                                   | CP   | 15   | 14   | 26   |        |
| 9 GCP<br>AP 1-12+<br>3 iteration  | GCPs | 4    | 10   | 11   | 1.20μm |
|                                   | CP   | 17   | 14   | 26   |        |
| 21 GCP<br>no AP                   | GCPs | 10   | 10   | 24   | 1.68μm |
|                                   | CP   | 13   | 16   | 41   |        |
| 21 GCP<br>AP 1-12                 | GCPs | 9    | 8    | 11   | 1.50μm |
|                                   | CP   | 13   | 15   | 26   |        |
| 21 GCP<br>AP 1-12 +<br>42-73      | GCPs | 8    | 8    | 10   | 1.31μm |
|                                   | CP   | 13   | 15   | 26   |        |
| 21 GCP<br>AP 1-12+<br>3 iteration | GCPs | 8    | 9    | 11   | 1.26μm |
|                                   | CP   | 13   | 16   | 26   |        |
| All GCP<br>no AP                  | GCPs | 13   | 14   | 68   | 1.58μm |
| All GCP<br>AP 1-12                | GCPs | 11   | 12   | 20   | 1.43μm |
| All GCP<br>AP 1-12 +<br>42-73     | GCPs | 11   | 12   | 18   | 1.24μm |

Table 1: results of bundle block adjustments  
 RMSX, RMSY, RMSZ [mm]  
 GCP = ground control points  
 CP = independent check points  
 + 3 iteration = 3 iterations with averaged residuals

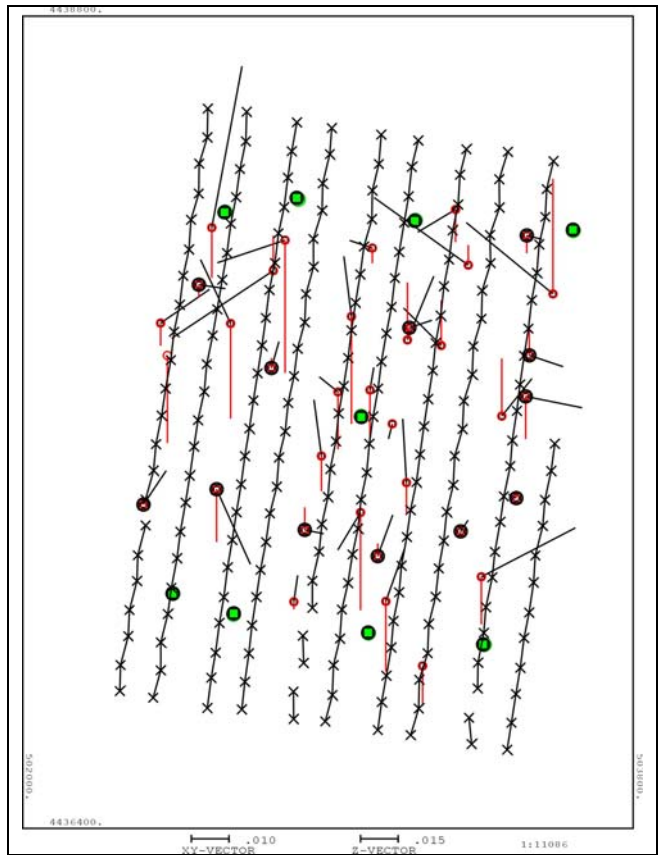


Fig. 16: control and check point configuration – green = control points

## 5. MODEL DEFORMATION

The systematic image errors are determined and respected in the block adjustment; here they are not causing any problem. In most cases this is different for the handling in the photogrammetric models, often the systematic image errors cannot be respected, but there is a trend to include the possibility of respecting the systematic image errors in commercial software. The model deformation caused by the systematic image errors should be checked at least.

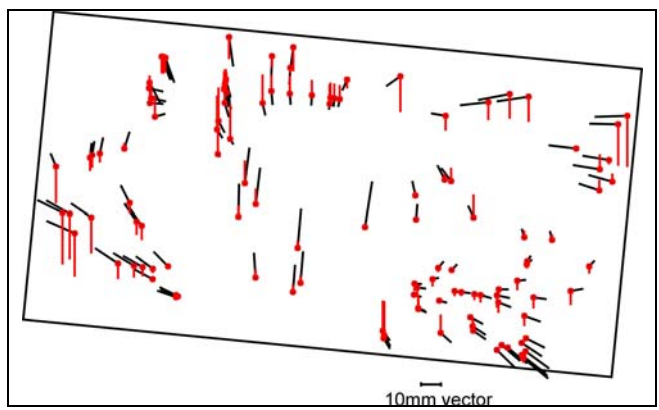


Fig. 17: Deformation of model 206/207 caused by systematic image errors, red vectors = Z-discrepancies

The deformation of the model 206/207 caused by systematic image errors can be seen in figure 17. The shown deformations are based on an optimal orientation of the deformed model. The root mean square discrepancies for X are 7mm, for Y 7mm and for Z 9mm with maximal discrepancies in X of 16mm, in Y 10mm and in Z 26mm. In relation to the reached accuracy the deformations are not negligible.

## 6. CONCLUSION

The extremely large scale digital aerial images having nominally 22mm GSD and effectively 25mm GSD are showing object details corresponding to aerial photos 1: 1250 under the condition of a scan of analog photos with 20 $\mu$ m pixel size. 20 $\mu$ m pixel size is the realistic resolution of analog photos in relation to digital images. Also analog photos with such a large scale are exceeding the image progress of 2seconds as the digital large frame images with nominally 22mm GSD. Opposite to the digital images the forward motion of analog images are exceeding the operational limits in such a case. Digital line scan cameras have not a sufficient sampling rate for reaching such a small GSD, so only with large format digital cameras a nominal GSD of 22mm is possible. Of course every flight line has to be flown twice to reach 60% end lap.

As shown in the figures 2 up to 4, with effectively 25mm GSD very small details can be identified. Any power line can be seen and not only manholes, but also details about the manholes can be identified.

The geometric object point accuracy reached in this test in the range of 0.6 GSD for X and Y and 1.2 GSD for independent check points, determined in the average by 6 images is at the level of the check point accuracy. It is totally satisfying for detailed mapping. As also shown before (Passini, Jacobsen 2008), the systematic image errors of the UltraCamX require a block adjustment with self calibration by additional parameters. For the limited size of the test area the UltraCam-specific additional parameters could not improve the results as well as with an iterative improvement of the image coordinates by overlaid and averaged residuals. The absolutely very high object point accuracy of a standard deviation of 14mm for the horizontal coordinate components and 26mm in Z could not be improved by direct sensor orientation.

## REFERENCES

- Passini, R., Jacobsen, K., 2008: Accuracy analysis of large size digital aerial cameras, International Archives of Photogrammetry, Remote Sensing and Spatial Information Sciences, Vol. XXXVII, Part B1 (WG I/4) pp 507-514
- Jacobsen, K., (2007): Geometric Handling of Large Size Digital Airborne Frame Camera Images, Optical 3D Measurement Techniques VIII, Zürich 2007, pp 164 – 171
- Jacobsen, K. (2008): Tells the number of pixels the truth? – Effective Resolution of Large Size Digital Frame Cameras, ASPRS 2008 annual convention, on CD